J. Fluid Mech. (2007), *vol.* 577, *pp.* 417–442.
doi:10.1017/S0022112007004636 Printed in the United Kingdom

The effect of wall heating on instability of channel flow

A. SAMEEN AND RAMA GOVINDARAJAN

Engineering Mechanics Unit, Jawaharlal Nehru Centre for Advanced Scientific Research, Bangalore-560064, India

(Received 28 December 2005 and in revised form 31 October 2006)

A comprehensive study of the effect of wall heating or cooling on the linear, transient and secondary growth of instability in channel flow is conducted. The effect of viscosity stratification, heat diffusivity and of buoyancy are estimated separately, with some unexpected results. From linear stability results, it has been accepted that heat diffusivity does not affect stability. However, we show that realistic Prandtl numbers cause a transient growth of disturbances that is an order of magnitude higher than at zero Prandtl number. Buoyancy, even at fairly low levels, gives rise to high levels of subcritical energy growth. Unusually for transient growth, both of these are spanwise-independent and not in the form of streamwise vortices. At moderate Grashof numbers, exponential growth dominates, with distinct Poiseuille–Rayleigh–Bénard and Tollmien–Schlichting modes for Grashof numbers up to $\sim$25 000, which merge thereafter. Wall heating has a converse effect on the secondary instability compared to the primary instability, destabilizing significantly when viscosity decreases towards the wall. It is hoped that the work will motivate experimental and numerical efforts to understand the role of wall heating in the control of channel and pipe flows.

1. Introduction

One of the well-known methods for delaying a transition to turbulence, for example in boundary layers, has been to reduce the viscosity at the wall. Such a reduction could be brought about by heating or cooling the surface, for example. The objective of this paper is to study the effect of wall heating on the instability of a channel flow. It is shown that heat can have surprising effects on the different mechanisms of transition. We restrict ourselves here to routes based on the linear eigenmodes, a direct nonlinear interaction will be studied in future. The emphasis here is on delaying/advancing the onset of transition to turbulence, rather than drag reduction in full turbulence, as achieved by adding small quantities of polymer.

In the linear regime, the early boundary-layer experiments of Wazzan, Okamura & Smith (1968) in water and Liepmann & Fila (1947) in air reported stabilization by heating and cooling, respectively. Several other experiments were carried out later to confirm these findings. For example, Lauchle & Gurney (1984) showed that the transition Reynolds number is increased by over an order of magnitude by heating the walls of an axisymmetric body in a water tunnel. The picture can be quite different in channel flow. The critical Reynolds number for linear instability in a plane Poiseuille flow is 5772.22 (Orszag 1971). However, experiments usually find fully developed turbulence at a much lower Reynolds number, around 1500 (see e.g. Davies & White 1928; Narayanan & Narayanan 1967; Patel & Head 1969; Kao & Park 1970). It

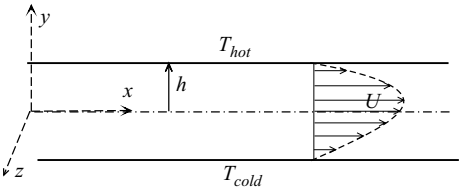

FIGURE 1. Schematic diagram of the channel, asymmetric heating. The two walls are held at different temperatures, T_{hot} and T_{cold}, so the mean temperature profile is linear. For buoyancy affected flows, gravity is taken to be along y, downwards for stable stratification.

is clear that routes to turbulence other than the traditional Tollmien–Schlichting (TS) mechanism are in operation. The background noise in the flow has a major influence in delaying/hastening transition to turbulence, as well as in deciding which mechanism will be dominant (Morkovin & Reshotko 1989). At extremely low levels of noise a traditional TS mechanism and/or secondary instability is likely to be followed. At intermediate levels, a transient growth of disturbances is the more likely mechanism for initial disturbance growth (Foster 1997; Corbett & Bottaro 2001; Schmid & Henningson 2001; Meseguer 2002). Once disturbance growth is triggered by a linear mechanism, nonlinearities are required to achieve a new self-sustained state. Alternatively, at higher levels of background noise, nonlinear mechanisms can directly come into play (see e.g. Waleffe 1997; Faisst & Eckhardt 2003; Hof *et al.* 2004). At present, it is not understood exactly which route will be followed when (for a review on pipe flow see Kerswell 2005).

As mentioned above, several workers have studied the effect of wall heating on linear stability alone. Here too, the effect of buoyancy has not been clearly quantified. To our knowledge, a detailed study of other mechanisms has not been done. Two related studies of transient growth had different emphasis from the present work: (Malik & Hooper 2005) evaluated the transient growth in two-fluid flow in two-dimensions with the objective of understanding the effect of the interface; Biau & Bottaro (2004) studied transient growth with stable thermal stratification and concluded that such stratification is a viable strategy to control transitional flows. A more detailed retrospective on earlier work is included in the relevant sections later in the text.

We consider two types of heating, as discussed in detail in § 2. The first is asymmetric, with the two walls maintained at different constant temperatures. The second is symmetric, with the walls at one temperature and the fluid at another, and is presented mainly to contrast with the results of the first. In each case we study the linear instability, the transient growth and the secondary instability. Heat can affect the stability of the flow because of the resulting mean viscosity stratification, or through temperature perturbations, and at levels of heating, through buoyancy. We consider each of these effects separately. We present results only at some typical values of the relevant parameter, such as the Reynolds number or the temperature difference. However, a much larger range of the parameter space has been explored and the results are representative. In wavenumber space, the emphasis where necessary, is on the least stable region.

2. Basic velocity profiles

Two types of temperature variation, which we shall refer to as the asymmetrically and symmetrically heated cases, respectively, are considered (figures 1 and 2). The

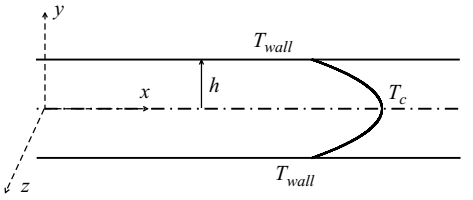

FIGURE 2. Schematic diagram of the channel, symmetric heating. Both walls are maintained at the same temperature, different from that of the fluid.

second is used here mainly for the purpose, of comparison with the first, but the two cases provide a fair sample of the type of stratification we may come across. In the first, the two walls of the channel are maintained at different temperatures, T_{hot} and T_{cold}. At steady state, the temperature within the channel varies linearly between the two. Note that for the unstable Poiseuille–Rayleigh–Bénard configuration, the temperature difference ΔT between the bottom and top walls (and hence the corresponding Richardson and Grashof numbers, defined later) is taken to be positive. The sign of ΔT is unimportant when buoyancy is neglected.

In the above flow, the temperature decreases away from one wall and increases away from the other. The effect on the two walls may thus be of opposing sign. To bring physical arguments to bear on the problem, it is useful to contrast the results we obtain with those obtained from a hypothetical symmetrically heated channel. Here, the walls are both maintained at the same temperature, while the incoming fluid is at a different temperature. The temperature profile would be of a developing error-function type, with the fluid temperature equilibrating eventually with the wall temperature. We present results taking the temperature to vary quadratically, but a local error-function profile did not give qualitatively different results. Since the Péclet numbers (the product of the Reynolds number and the Prandtl number) are high, the change in the downstream direction is very slow, and the flow may be assumed to be locally parallel.

The temperature-dependence of the viscosity μ is described by the Arrhenius model, which works fairly well for most common liquids such as water and alcohol:

$$\mu_d(T) = C_1 \exp(C_2/T), \tag{2.1}$$

where μ is the dynamic viscosity (the subscript d stands for a dimensional quantity) T is the temperature, C_1 and C_2 are constants associated with the fluid under consideration, which is taken in the present computations to be water, i.e. we set $C_1 = 0.00183\,\mathrm{Ns\,m^{-2}}$ and $C_2 = 1879.9\,\mathrm{K}$ (see e.g. Lide 1999). Without loss of generality, the temperature at the cold wall is taken to be 295 K. We have found that changes in these numbers do not affect results qualitatively.

The streamwise direction is denoted as x, the coordinate y is normal to the wall, and z is the spanwise direction. The mean x-momentum equation for a plane parallel channel flow reduces to

$$(\mu U')' = \frac{\mathrm{d}P}{\mathrm{d}x} Re_f, \tag{2.2}$$

where the primes denote differentiation with respect to y. A subscript f is used in the above Reynolds number, defined as $Re_f = U_{max} h\rho/\mu_{ref}$ to distinguish it from the Reynolds number Re defined later in terms of the average viscosity. h is the half-channel width, ρ is the density, and $\mathrm{d}P/\mathrm{d}x$ is the constant mean pressure gradient. The effect of buoyancy is studied under the Boussinesq approximation, and ρ is taken

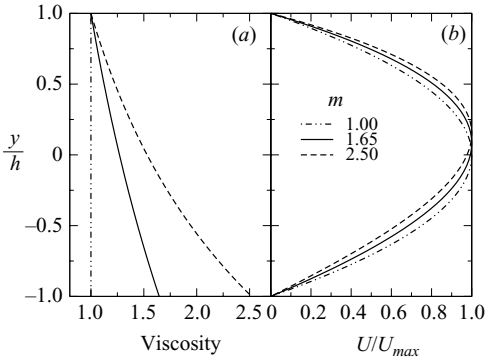

FIGURE 3. Variation of (*a*) viscosity and (*b*) velocity with asymmetric heating. The velocity is scaled by its maximum and the viscosity is scaled here by its value at the hot wall.

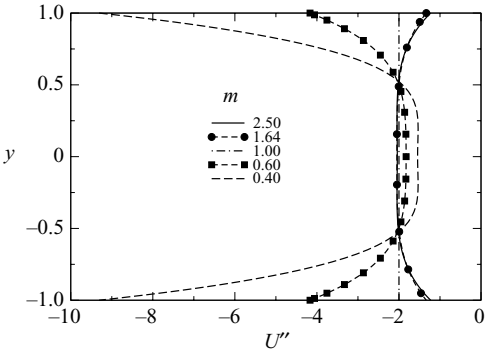

FIGURE 4. Variation of the second derivative of basic velocity, U'', with symmetric heating.

to be constant except in the acceleration term. μ_{ref} is the reference viscosity, at the hot wall for asymmetric heating, and at the centreline for symmetric heating. The quantity $\mu \equiv \mu_d/\mu_{ref}$, and we define a viscosity ratio $m \equiv \mu_{cold}/\mu_{ref}$ for the asymmetric heated case and $m \equiv \mu_{wall}/\mu_{ref}$, for the symmetric case. Knowing $\mu(T)$ and $T(y)$, equation (2.2) is integrated twice by a fourth-order Runge–Kutta method to obtain U. Figure 3 shows typical viscosity and velocity profiles for asymmetric heating. For the symmetric case, the effect of viscosity stratification on the velocity profile is more evident in its second derivative, which is shown in figure 4.

Unless otherwise specified, the Reynolds number is defined in terms of the average viscosity across the channel, as

$$Re \equiv \frac{2}{\displaystyle\int_{-1}^{1} \mu \, \mathrm{d}y} \frac{U_{max} h \rho}{\mu_{ref}}, \tag{2.3}$$

We can see from table 1 that the average viscosity varies significantly with increasing ΔT, so defining the Reynolds number as above is approriate for making comparisons at a given Reynolds number between heated and unheated flows. The average velocity on the other hand is practically unchanged by viscosity stratification, as seen from the same table, so the maximum velocity is a good enough velocity scale.

ΔT (K)	m	$\mu_{avg} = \frac{1}{2}\int_{-1}^{1} \mu \, \mathrm{d}y$	$U_{avg}/U_{avg,m=1.0}$
50	0.39	0.748	1.068
10	0.81	0.933	1.006
0.0	1.00	1.000	1.000
−10	1.23	1.070	0.995
−50	2.51	1.381	0.9944

TABLE 1. The dependence of the average viscosity μ_{avg} on the viscosity ratio, m, symmetric heating. The right-hand column shows the ratio of the average mean velocity to its value in the unheated case. The ratio is close to 1.0 in all cases.

3. Linear stability

3.1. *The stability equations and their solution*

The equations for linear stability are derived by the standard procedure. Each flow quantity is split into its mean and a perturbation. The perturbation quantities in normal mode form are given as

$$[\hat{v}, \hat{\eta}, \tilde{T}] = [v(y), \eta(y), \hat{T}(y)] \exp[\mathrm{i}(\alpha x + \beta z - \omega t)], \tag{3.1}$$

where $\hat{v}$ and $\hat{\eta}$, respectively, are the components of disturbance velocity and vorticity in the direction normal to the wall, $\tilde{T}$ is the disturbance temperature, α and β are the wavenumbers in the streamwise and spanwise directions, respectively, and ω is the complex frequency of the wave. Substituting the flow quantities thus defined into the momentum and continuity equations, subtracting the basic flow equations, and neglecting nonlinear terms in the perturbation quantities, the linear stability equations are derived to be

$$\begin{aligned}
\mathrm{i}\alpha[(v'' - (\alpha^2+\beta^2))(U-c) - U''v] = \frac{1}{Re}\Bigg[&\mu[v^{\mathrm{iv}} - 2(\alpha^2+\beta^2)v'' + (\alpha^2+\beta^2)^2 v] \\
&+ \frac{\mathrm{d}\mu}{\mathrm{d}T}T'2[v''' - (\alpha^2+\beta^2)v'] + \frac{\mathrm{d}\mu}{\mathrm{d}T}T''[v'' + (\alpha^2+\beta^2)v] + \frac{\mathrm{d}^2\mu}{\mathrm{d}T^2}T''[v'' + (\alpha^2+\beta^2)v] \\
&+ \frac{\mathrm{d}\mu}{\mathrm{d}T}[U'\hat{T}'' + 2U''\hat{T}' + (\alpha^2 U' + U''')\hat{T}] + 2\frac{\mathrm{d}^2\mu}{\mathrm{d}T^2}U'T'\hat{T}' + \frac{\mathrm{d}^2\mu}{\mathrm{d}T^2}T''U'\hat{T} \\
&+ \frac{\mathrm{d}^3\mu}{\mathrm{d}T^3}U'T'\hat{T} - \frac{Gr}{Re}\mathrm{i}\alpha\hat{T}\Bigg],
\end{aligned} \tag{3.2}$$

$$\begin{aligned}
\mathrm{i}\alpha(U-c)\eta + \mathrm{i}\beta U'v = \frac{1}{Re}\Bigg[&\mu[\eta'' - (\alpha^2+\beta^2)\eta] + \frac{\mathrm{d}\mu}{\mathrm{d}T}T'\eta' - \mathrm{i}\beta\frac{\mathrm{d}\mu}{\mathrm{d}T}(U''\hat{T} + U'\hat{T}') \\
&- \mathrm{i}\frac{\mathrm{d}^2\mu}{\mathrm{d}T^2}T'U'\hat{T}\Bigg],
\end{aligned} \tag{3.3}$$

$$\mathrm{i}\alpha(U-c)\hat{T} + T'v = \frac{1}{RePr}[\hat{T}'' - (\alpha^2+\beta^2)\hat{T}], \tag{3.4}$$

where $c \equiv \omega/\alpha$. The Prandtl number is defined as $Pr \equiv \nu/\kappa$ where κ is the coefficient of thermal diffusivity, and the kinematic viscosity here is $\nu = \mu_{ref}/\rho$. The Grashof number is $Gr \equiv g\gamma\Delta T h^3/\nu^2$, g and γ being the acceleration due to gravity and the volume coefficient of expansion, respectively. The Boussinesq approximation has been employed.

The effect of heating appears in the stability equations (3.2) to (3.4) in three types of term. One set of terms appears because the mean viscosity μ is a function of the mean temperature, which in turn is a function of the distance y from the wall. The second effect comes from the viscosity stratification as well, but is due to the finite diffusivity of the temperature perturbations. If the Prandtl number were to be zero, the temperature perturbation obtained from (3.4) would be zero too. In other words, heat diffuses away infinitely fast and a non-zero $\hat{T}$ cannot be sustained. However as the Prandtl number increases, the temperature perturbations are larger, and may be expected to increasingly affect stability. A third effect of heat comes from the small variation in density arising from the variation in temperature. This exerts a buoyancy force, proportional to the Richardson number ($Ri \equiv Gr/Re^2$), appearing in (3.2). In what follows, each of these effects will be studied separately. If the equations above were stripped of these three effects, we would be left with the Orr–Sommerfeld and Squires equations for flow through a channel. If buoyancy alone were to be neglected, the equations would be equivalent to those of Wall & Wilson (1996).

Equations (3.2) to (3.4) form an eigenvalue problem with the boundary conditions

$$v(\pm 1) = v'(\pm 1) = \eta(\pm 1) = \hat{T}(\pm 1) = 0, \tag{3.5}$$

and are solved using a Chebyshev spectral collocation method (see Peyret 2002; Canuto *et al.* 1987 for the standard technique). We have performed computations with 81 and 161 collocation points across the channel, and the eigenvalues change only in the sixth decimal place at worst. For an unheated channel, the accuracy is much better and the eigenvalues agree up to seven decimal places with Schmid & Henningson (2001). Other accuracy checks are presented later in the paper. We perform a temporal stability analysis, where the growth rate of the disturbance is given by the imaginary part of ω.

3.2. *Effect of viscosity variation*

In order to isolate the effect of viscosity variation, the Prandtl number and the Grashof number are set to zero. The linear stability of boundary-layer flows with viscosity stratification has been studied by Kao (1968), Wazzan *et al.* (1968), Strazisar, Reshotko & Prahl (1977) and Schafer, Severin & Herwig (1995). It is well-established that a viscosity which decreases as one approaches the wall has a stabilizing effect on the least stable eigenmode. This is because such a viscosity stratification makes the velocity profile fuller, i.e. takes it further away from an inflectional profile. Since the viscosity of liquids decreases with heating, a liquid boundary layer at a hot wall is more stable, but the reverse is true of gases (Liepmann & Fila 1947). By the same argument, a viscosity increase towards the wall is destabilizing, and this too has been verified. In the flow through a channel with symmetric heating we therefore expect, and find in the hypothetical case we study, that wall heating ($m < 1$) will result in a more stable flow (figure 5).

However, in a channel flow where one wall is maintained at a constant high temperature and the other wall is kept cold, the viscosity decreases towards one wall and increases towards the other. It is not *a priori* evident what the effect on the linear stability will be. It was found by Potter & Graber (1972) that any temperature difference between the walls is always destabilizing. However, Wall & Wilson (1996) found, using four different viscosity models, that a temperature difference almost always stabilizes the flow. The apparent contradiction is because the former work compared results for heated and unheated flow maintaining the input power constant, whereas the latter made comparisons at a given Reynolds number. Since the flow

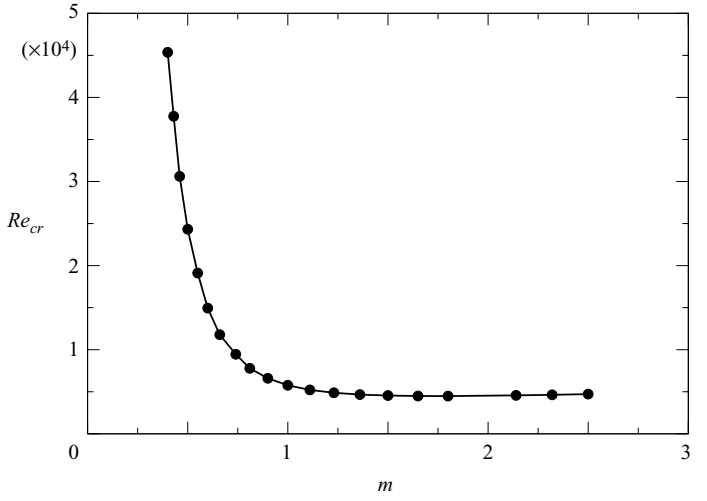

FIGURE 5. Effect of viscosity variation on the critical Reynolds number for linear instability, symmetric heating. For unstratified flow, i.e. at $m = 1.0$, Re_{cr} is 5772.2.

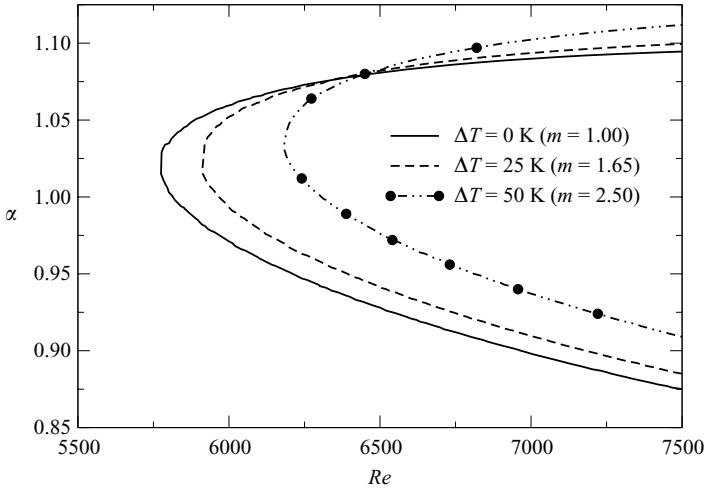

FIGURE 6. Stability boundaries for various viscosity ratios. Asymmetric heating, $T_{cold} = 295$ K.

rate for a given input power is higher for the heated case, the resulting Reynolds number is higher. The stability of viscosity-stratified channel flows was also studied by Pinarbasi & Liakopoulos (1995); Schafer & Herwig (1993) with conclusions similar to Wall & Wilson (1996).

In the present paper, we define the Reynolds number in terms of average viscosity, and compare results at a given Reynolds number. In agreement with Wall & Wilson (1996), for asymmetric heating, we find that any temperature difference is stabilizing, in terms of the least stable (two-dimensional) linear mode (figure 6). We have confirmed (Sameen 2004) that the production of disturbance kinetic energy is reduced at the cold wall and increased at the hot wall compared to the unheated case. The dissipation is similar in all cases. The highly oblique modes, unlike the two-dimensional ones, are

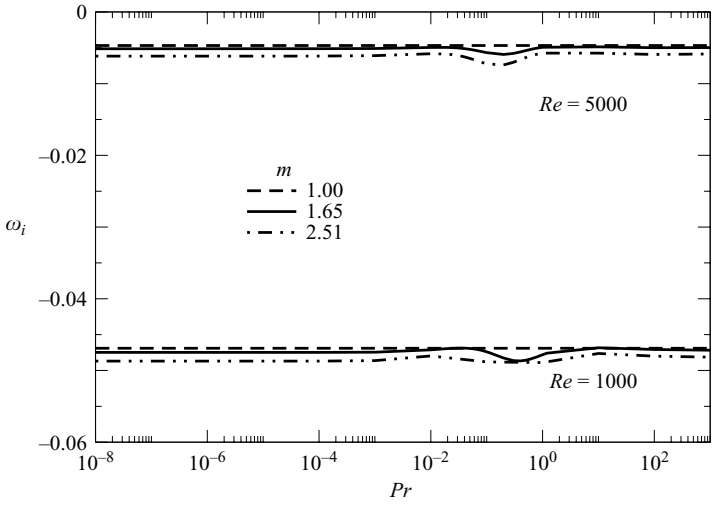

FIGURE 7. Least stable eigenvalue at various Prandtl numbers for different ΔT at $\alpha = 0.9$ and $Re = 1000$, 5000. The effect of Prandtl number is negligible.

practically unaffected (not shown). This observation will assume significance when we discuss transient growth.

3.3. *Effect of heat diffusivity*

We know that for liquids such as water, heat diffuses much slower than momentum, so the assumption of $Pr = 0$ is not justifiable. Surprisingly however, the linear stability, as measured by the least stable eigenmode, is practically unaffected by a decrease in heat diffusivity (Wall & Wilson 1996). Present computations confirm this (figure 7). However, the prevalent conclusion that heat diffusivity does not affect flow stability, and therefore that the Prandtl number may be set to zero in stability analyses, is shown in the next section to be incorrect. Increasing the Prandtl number to $O(1)$ values can enhance transient growth by an order of magnitude. We note a small but curious dip in the growth rate just below $Pr = 1$ in figure 7; what causes it is unclear at this time. Wall & Wilson (1996) too obtain a similar dip (see table 2 of that paper), and do not explain it either.

3.4. *Effect of buoyancy: the Poiseuille–Rayleigh–Bénard problem*

The relevant case for the study of buoyancy effects is the asymmetrically heated one. When the upper wall is cold relative to the lower one, the resulting unstable stratification of density leads, at low flow rates, to a buoyancy-driven instability similar to the Rayleigh–Bénard (Turner 1959; Chandrasekhar 1961; Platten & Legros 1984). The effect of mean shear on this instability has been studied by Deardorff (1965) and Zhang, Childress & Libchaber (1998), for example, and this problem is reviewed in Platten & Legros (1984) and Mahajan *et al.* (1988). This regime of instability is termed the Rayleigh–Bénard–Poiseuille (RBP) instability. Carriere & Monkewitz (1999) obtained stability boundaries for the RBP instability and showed that the flow at very low Reynolds numbers and high Grashof numbers is absolutely unstable. At a given Grashof number, the region of absolute instability is restricted to extremely low Reynolds numbers. For example, at $Gr = 2000$, the flow is absolutely unstable for Reynolds numbers below ~ 10.

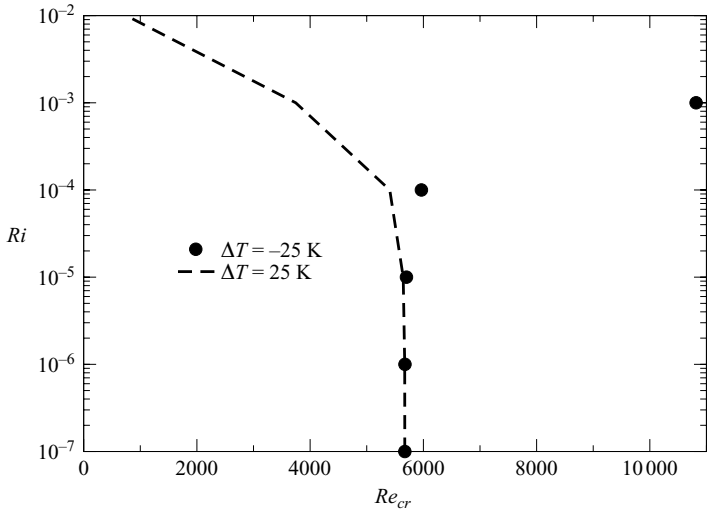

FIGURE 8. Neutral stability Reynolds number as a function of Richardson number, $Pr = 1.0$. For stable stratification ($\Delta T < 0$), the Richardson number is negative, its absolute value is plotted here. The portion to the right-hand side of the neutral points is unstable.

Our interest is in the regime of high flow rates, with Grashof numbers increasing from zero, so the present instability would come under the class of Poiseuille–Rayleigh–Bénard (PRB). The order of names is reversed to emphasize the reversal of relative magnitudes, and also the fact that the modes of instability are distinct. Such a situation has been investigated by Gage & Reid (1968), Gage (1971), Tveitereid (1974) and Fujimura & Kelly (1988). However, several approximations were made in these early studies. For example, viscosity variations were neglected and the base flow was taken to be parabolic. It was found that a critical Reynolds number always exists for any level of density stabilization, while there exists a Richardson number above which the flow is stable for all Reynolds numbers.

In figure 8, the critical Reynolds number, Re_{cr} for a temperature difference of 25 K is plotted for various Richardson numbers. The trends are the same as in Gage & Reid (1968) and Tveitereid (1974), but there are minor numerical discrepancies, which we attribute to the more appropriate velocity and viscosity profiles used here. The effects of buoyancy are negligible when the Richardson number is below 10^{-4}, and of either sign. At higher Richardson numbers, for unstable stratification, figure 8 shows that the flow is highly destabilized. The stability boundaries are plotted in figure 9 in terms of the Grashof number, a given Grashof number being more simple to achieve experimentally. Distinct modes of PRB type and of Poiseuille (or TS) type are evident at intermediate levels of Gr. Increasing levels of buoyancy destabilize the TS mode as well, so that the PRB and TS modes merge at Grashof numbers above $\sim$25 000. The numerical value at the bifurcation point varies slightly with Prandtl number and temperature difference.

The stability boundary is shown in the Grashof–Reynolds parameter space in figure 10. The region of PRB instability is seen to occur only at Reynolds numbers $O(100)$ or higher, and the boundary is closed (figure 9) at low Grashof numbers, so it is clearly distinct from the RBP mode of Carriere & Monkewitz (1999) at the same Prandtl number. Since the results of Carriere & Monkewitz (1999) for convective instability are restricted to Reynolds numbers below 15, the upper bound for the

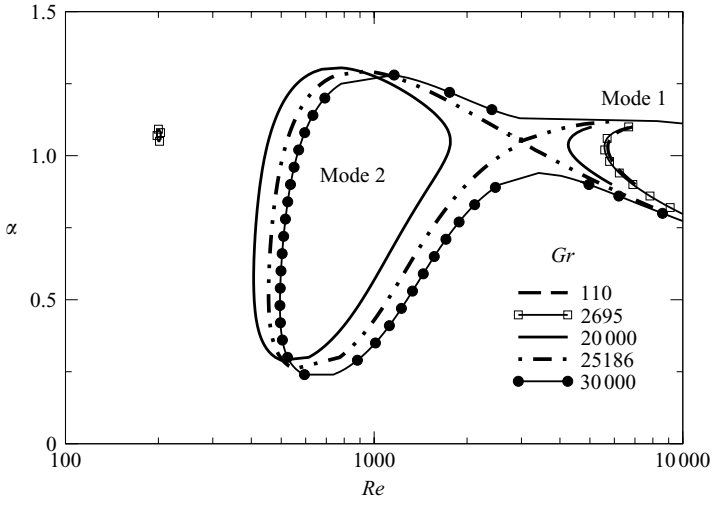

FIGURE 9. The neutral curves for unstably thermal stratified flow at Prandtl number 7.0, $\Delta T = 25\,\mathrm{K}$. The Poiseuille–Rayleigh–Bénard mode starts appearing at $Gr = 2695$ and merges with the Poiseuille mode at $Gr = 25\,186$.

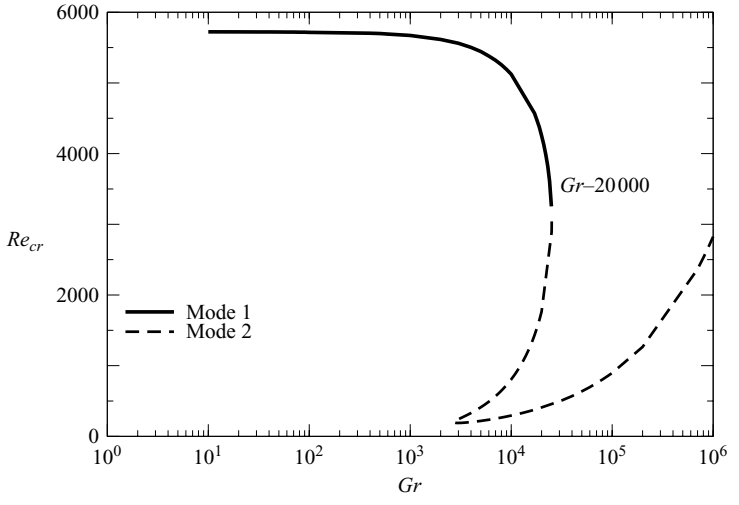

FIGURE 10. A consolidated picture of the variation of the critical Reynolds number with the Grashof number. The Poiseuille mode is shown by the solid line, and the Poiseuille–Rayleigh–Bénard mode by the dashed line. The region above the curves is unstable.

RBP mode is not evident, but visual extrapolation of the available curve indicates a closure at Reynolds numbers much lower than those of present interest, at a given Gr. In the Reynolds-number range studied here, i.e. $O(10^2)$ to $O(10^4)$, we expect that the flow will be only convectively unstable. However, a search for absolute instabilities, especially above the bend in the dashed line in figure 10 may yield interesting results.

We have discussed the stability in terms of the most unstable linear mode. However, a transient growth of decaying modes can often be the dominant mechanism of transition to turbulence in channel flows. We shall see in the next section that the effect of heat on flow instability throws up several surprises.

4. Transient growth

As mentioned in § 1, the typical flow through a channel goes through a transition to turbulence at a Reynolds number far below the critical value for linear instability. The mechanism of transition, except in extremely quiet flows, is thought to be due to a combination of transient growth (in the initial stages) and nonlinearlity (Morkovin & Reshotko 1989). In this study, we evaluate the effect of heating on the former, namely, transient or algebraic growth of disturbances. Transient growth occurs because even while all individual disturbance eigenmodes are exponentially decaying, they can superimpose linearly to give fairly large levels of growth over finite periods of time (Landahl 1980). If the entire process were to be linear, then at very large times, the exponential decay would dominate and the flow would resume its original state. However, if the transient disturbance amplitudes attained are sufficient to trigger nonlinearities and the self-sustaining mechanism of vortex generation (Waleffe 1995, 1997), the flow can become turbulent. A necessary condition for the different modes to superimpose in this manner is, of course, that the eigenfunctions should not be orthogonal (Schmid & Henningson 2001; Criminale, Jackson & Joslin 2003). The fact that the linear stability operator is not self-adjoint ensures that this is the case. In wall-bounded flows, transient growth is mainly caused by the interaction between the Orr–Sommerfeld and Squire modes (Reddy & Henningson 1993; Criminale *et al.* 2003) from the coupling term, $-\mathrm{i}\beta U'$, appearing in Squire's equation. The most likely structures arising owing to transient growth in unheated flows are streamwise streaks (Reddy *et al.* 1998; Reddy & Henningson 1993, 1994; Schmid & Henningson 2001). We use the standard approach for computing the maximum transient growth, details are available in, for example, Schmid & Henningson (2001).

The effect of viscosity-stratification on transient growth, in contexts other than heat (Malik & Hooper 2005; Chikkadi, Sameen & Govindarajan 2005) has been addressed before, though not completely. The effect of buoyancy has been studied under stable stratification alone by Biau & Bottaro (2004). The effect of heat diffusivity on transient growth has not been studied before, to our knowledge.

The disturbance energy, $g(t)$ (Schmid & Henningson 2001), is written as

$$g(t) = \frac{\|\kappa(t)\|_E^2}{\|\kappa(0)\|_E^2} = \frac{\|\mathrm{e}^{-\mathrm{i}\Lambda t}\kappa(0)\|_E^2}{\|\kappa(0)\|_E^2}. \tag{4.1}$$

Its time evolution is represented by the matrix $\partial\kappa/\partial t = -\mathrm{i}\Lambda\kappa$, where $\kappa = (\kappa_1, \kappa_2, ..., \kappa_N)^T$ and $\Lambda = \mathrm{diag}\{\omega_1, \omega_2, ..., \omega_N\}$, κ_j is the jth expansion coefficient of the eigenfunctions of the linear modes which are the dominant contributors here. The superscript T denotes transpose. The norm used in (4.1) is defined in the following paragraphs.

A representative measure of transient energy growth remains to be defined. For the case of zero Prandtl number, the density of disturbance kinetic energy is a meaningful measure. In (3.2) to (3.4), as the Prandtl number increases the contribution to the stability of the temperature fluctuations, $\hat{T}$ will increase. For realistic Prandtl numbers, the relevant measure of disturbance 'energy' is defined to be (see e.g. Hanifi, Schmid & Henningson 1996; Carriere & Monkewitz 1999) of the form

$$E = \iiint A(u_i^* u_i + v_i^* v_i + w_i^* w_i) + B(\hat{T}^* \hat{T})\,\mathrm{d}x\,\mathrm{d}y\,\mathrm{d}z, \tag{4.2}$$

where $*$ denotes the complex conjugate. Since we are interested only in relative growth, one of the coefficients, e.g. A, may be set to 1. For fixed spanwise and streamwise

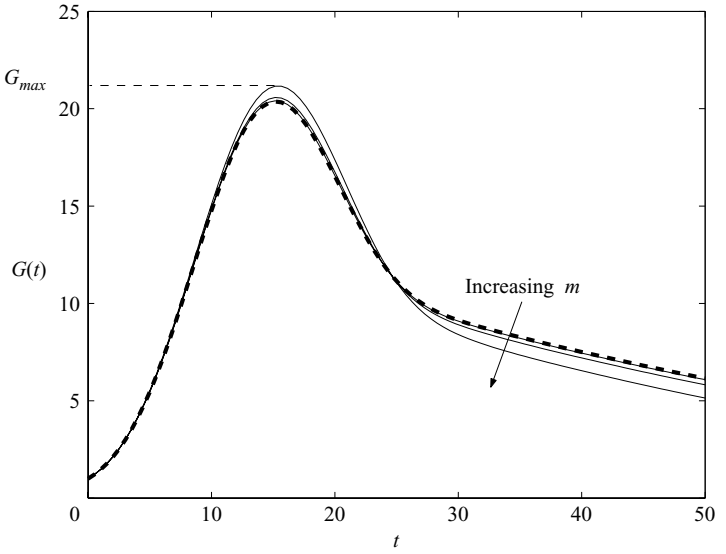

FIGURE 11. The energy amplification evolution for various viscosity ratios for $Re = 3000$, $\alpha = 1$, asymmetric heating. The thick dashed curve is for unstratified flow, and the solid lines are for $m = 1.2$, 1.65 and 2.5 in the order indicated in the figure.

81 collocation points			161 collocation points		
G_{max}	t_{max}	m	G_{max}	t_{max}	m
196.001715	76.668427	1.00	196.001746	76.668439	1.00
196.841804	76.698949	1.49	196.841820	76.698956	1.49
198.671305	76.819408	1.96	198.671276	76.819395	1.96
201.396974	77.021089	2.51	201.396969	77.021087	2.51

TABLE 2. Comparison of results using 81 and 161 collocation points. The time at which the maximum amplitude G_{max} is attained is shown as t_{max}. Representative results at $\alpha = 0.0$, $\beta = 2.0$, $Re = 1000$ and $Pr = 0$ for the asymmetric profile are shown, but the accuracy is at least as good over the entire parameter range.

wavenumbers, the integrals in these coordinates scale out of the problem, so

$$E = \int |u|^2 + |v|^2 + |w|^2 + B|\hat{T}|^2 \, \mathrm{d}y. \tag{4.3}$$

The coefficient B is a positive definite scalar, but arbitrary. A specific choice of B will, of course, change the norm quantitatively, but the findings are not expected to change qualitatively (Hanifi & Henningson 1998; Biau & Bottaro 2004). This assertion is evaluated at the end of this section, but as in earlier work, we present results for $B = 1$.

Maximizing equation (4.1) for all possible initial conditions $\kappa(0)$, we have

$$G(t) = \max_{\kappa \neq 0} g(t). \tag{4.4}$$

We then define G_{max} as the maximum over time of $G(t)$ for one particular set of Re, α, β and ΔT (see figure 11). A comparison between the results from 81 and 161 collocation points in table 2 shows that 81 collocation points are sufficient to

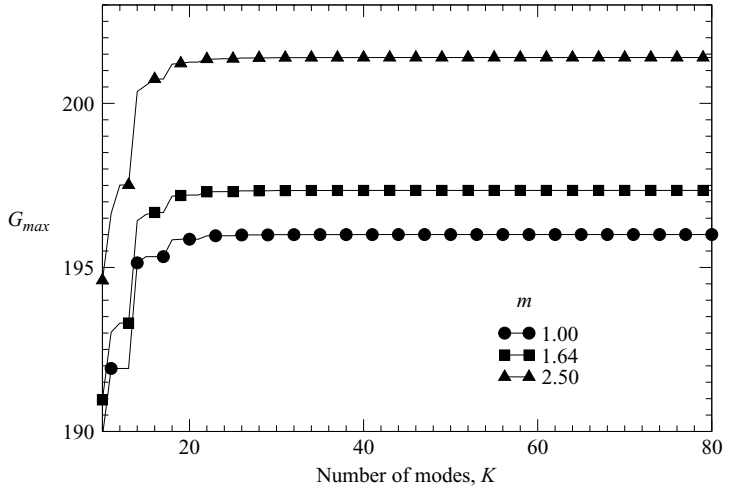

FIGURE 12. Dependence of G_{max} on the number of modes taken into consideration for the computations of transient growth. Asymmetric case, $Re = 1000$, $\beta = 2$ and $\alpha = 0$.

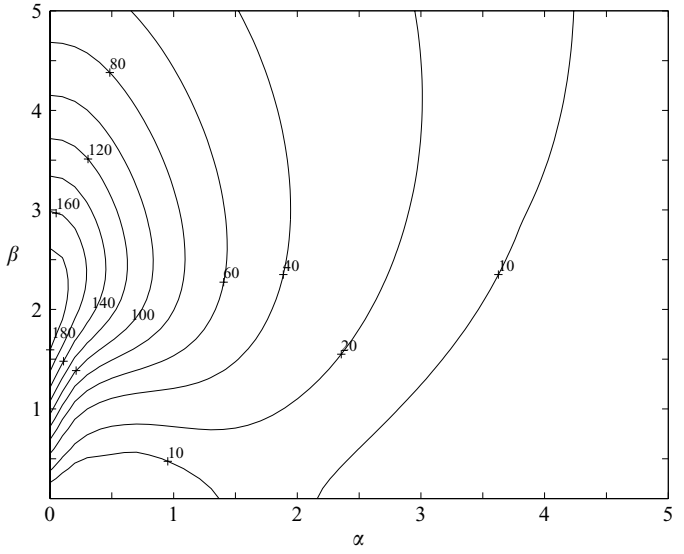

FIGURE 13. The contour of G_{max} (the maximum over time of $G(t)$) for $Re = 1000$ in the (α, β)-plane, $\Delta T = 0\,\mathrm{K}$. This matches well with Reddy & Henningson (1993).

give accurate results for G_{max} and the corresponding time at which it occurs, at any viscosity ratio. The computed transient growth of the optimal perturbation will, in principle, depend on the number N of eigenmodes taken into consideration, so it must be ensured that all the contributing modes are included in the computation. The dependence of G_{max} on the number of modes is shown in figure 12. As seen, the contribution of additional modes beyond $j \sim 25$ is negligible. The contour plot for G_{max} for unheated flow is shown at $Re = 1000$ in figure 13, for comparison with the results for heated flow to follow. A maximum growth of $G_{max} = 196$ is obtained for $\alpha = 0.0$ and $\beta = 2.05$ (see Reddy & Henningson 1993).

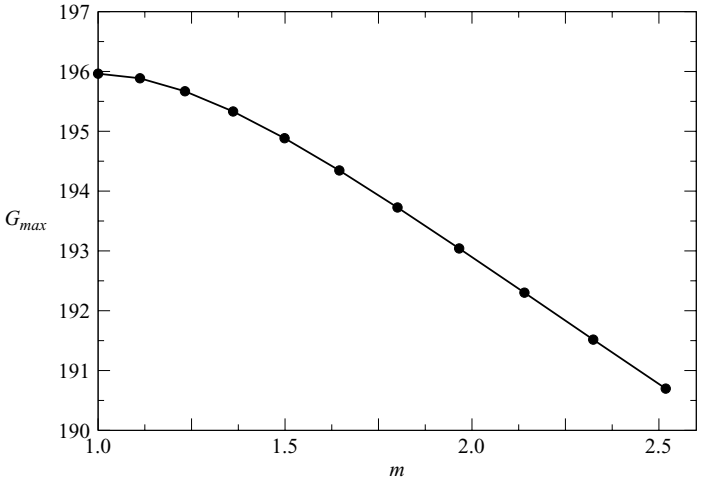

FIGURE 14. The variation of G_{max} at $\alpha = 0$ and $\beta = 2$ for various viscosity ratios at $Re = 1000$, asymmetric heating. The maximum deviation of G_{max} from the unheated value of 196 is only 3%.

4.1. *Effect of viscosity stratification*

As before, we first take the Prandtl number to be zero, i.e. assume that temperature fluctuations diffuse away instantaneously. We also neglect buoyancy, in order to isolate the effect of viscosity stratification alone. For the asymmetrically heated case, the growth of kinetic energy is seen in figure 11 to change only marginally with heating. The example shown in figure 11 is for $Re = 3000$ and $\alpha = 1$. We have made similar computations for a wide range of Reynolds numbers, wavenumbers and temperature difference, and verified that a stratification of viscosity has very little effect on transient growth for any configuration. The effect of asymmetric heating is quantified in figure 14 in terms of G_{max} at $\alpha = 0$ and $\beta = 2$. There is a marginal stabilization with viscosity stratification. This result is in line with the result for linear stability, but much smaller in magnitude. For comparison, the variation of G_{max}, again at $\alpha = 0$ and $\beta = 2$, for symmetric heating is plotted in figure 15. Here too there is a slight stabilization with increase in viscosity stratification.

The insignificant effect of viscosity stratification is consistent with our study of transient growth in two-fluid and non-Newtonian flows (Chikkadi *et al.* 2005). As discussed there, the U'' term, which affects the least stable eigenmode dramatically, has no effect on streamwise vortices arising from $\alpha = 0$, which dictate transient growth. The eigenspectrum, and typical eigenfunctions at $\alpha = 0$ are shown in figure 16 to be very similar at two extremes of viscosity stratification. Equation (3.3) drives the dynamics rather than equation (3.2) under these conditions, and the terms containing viscosity gradients have been verified numerically to be small.

4.2. *Effect of heat diffusivity*

It has been seen that the Prandtl number has a marginal effect on the most unstable linear mode. In contrast, we find here that reducing heat diffusivity has a large destabilizing effect on the transient growth of disturbance kinetic energy. In figure 17, for a temperature difference of 25 K at a Reynolds number of 1000, the effect of Prandtl number is shown. As the Prandtl number is increased from 10^{-4} to 1, the transient growth is seen to increase dramatically. The large destabilization comes

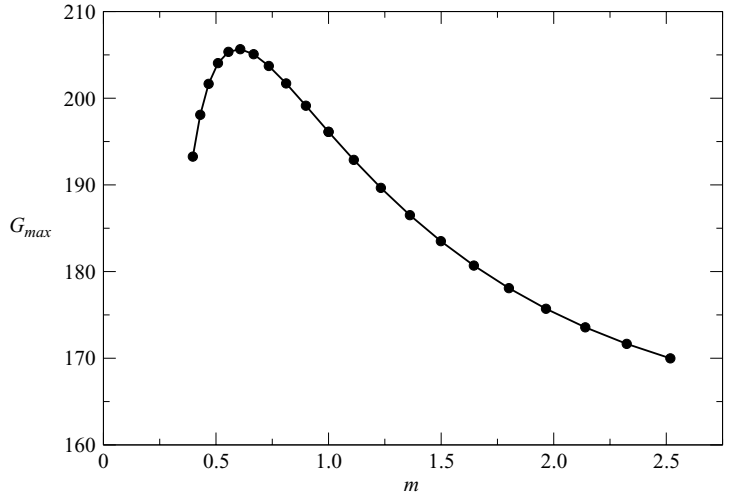

FIGURE 15. The G_{max} variation at $\alpha = 0.0$ and $\beta = 2.0$ for various viscosity ratios at $Re = 1000$, symmetric heating. The maximum deviation of G_{max} from that for unstratified flow is only 13%.

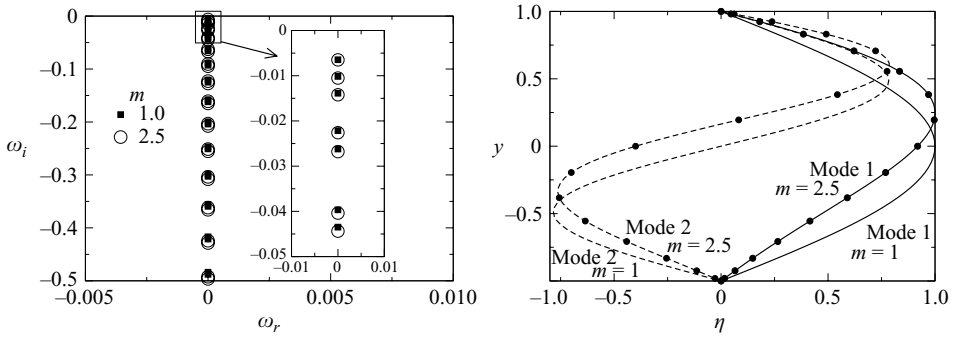

FIGURE 16. (*a*) The eigenspectra for two extremes of viscosity stratification, $m = 1$ and 2.5, for $\alpha = 0$, $Re = 1000$ and $\beta = 2.0$, asymmetric heating. (*b*) The corresponding eigenfunctions of the first two unstable eigenvalues in each case.

from a new region in the (α, β)-space, which is nearly two-dimensional. This is true for symmetric heating as well (not shown). The result is qualitatively the same for other temperature differences as well. We now have a situation where transient growth dominates, but not via the standard streamwise streaks and streamwise vortices.

4.3. *Effect of unstable density stratification*

In their studies of stable thermal stratification, Biau & Bottaro (2004) have found that as stratification increases, flow becomes increasingly stable, both in terms of exponential growth and transient growth. Viscosity variations were not accounted for in their calculation. In this paper, we concentrate on unstable thermal stratification.

Figures 18 to 21 show contour plots of maximum growth of transient energy for various Grashof numbers at increasing Prandtl number for a temperature difference of $\Delta T = 25\,\mathrm{K}$. As expected, when heat diffusivity is high, buoyancy has little effect.

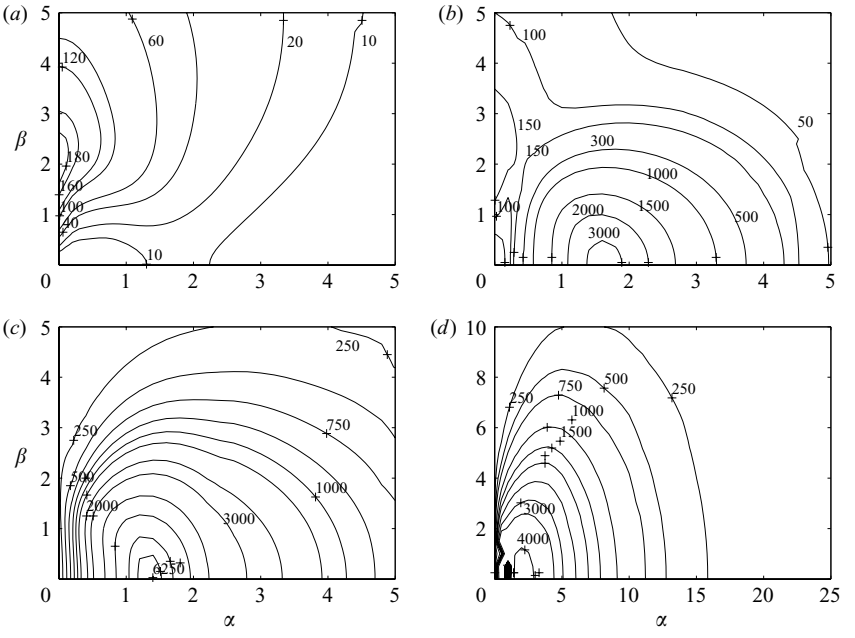

FIGURE 17. Contour plot of G_{max} for $T = 25\,\mathrm{K}$ (asymmetric), $Re = 1000$ for various Prandtl numbers. (*a*) $Pr = 10^{-4}$, (*b*) 10^{-2}, (*c*) 10^{-1}, (*d*) 1. Note that in (*d*) the scale employed is different.

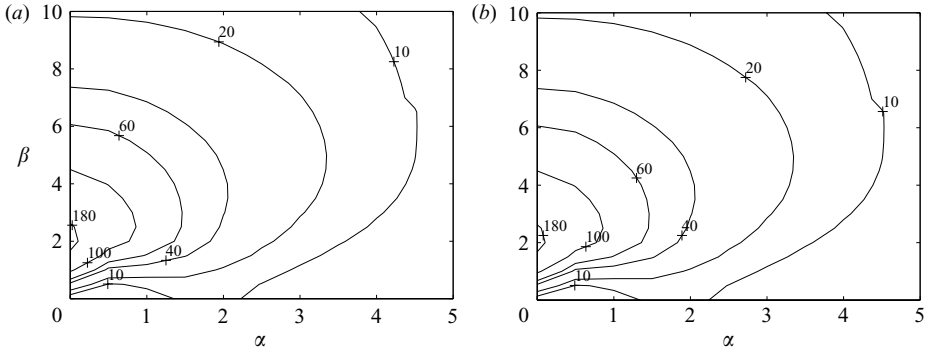

FIGURE 18. The transient growth at (*a*) $Gr = 1$, (*b*) $Gr = 10^4$ for $\Delta T = 25\,\mathrm{K}$, $Re = 1000$ and $Pr = 10^{-4}$ with asymmetric heating. Since temperature perturbations diffuse away rapidly, buoyancy does not have much effect.

For $Pr \leqslant 0.01$, the Prandtl number dictates the instability, and buoyancy has very little effect. At $Pr = 1$, however, the situation is completely different. For Grashof numbers of 1000 and below, we see extremely large levels of subcritical transient growth. This growth is two-dimensional. Above this Grashof number of course, a linearly unstable mode exists. The transient growth in unheated channel flow is well known to display itself as streamwise-independent structures, such as streaks and vortices. Our results indicate that such structures will not be much in evidence in heated flows at realistic Prandtl or Grashof numbers. Rather, a spanwise-independent growth occurs. Experimental and numerical verification of this kind of transient growth could have consequences for wall heating as a control option.

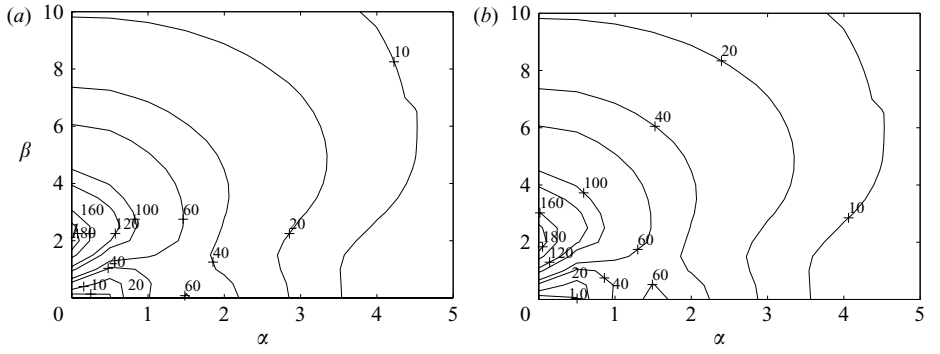

FIGURE 19. As figure 18, but for $Pr = 10^{-3}$. The Grashof number has no effect up to a value of $\sim 10^4$. At $Gr = 10^4$ a new growth appears at $\beta = 0$, which will dominate at higher Prandtl number.

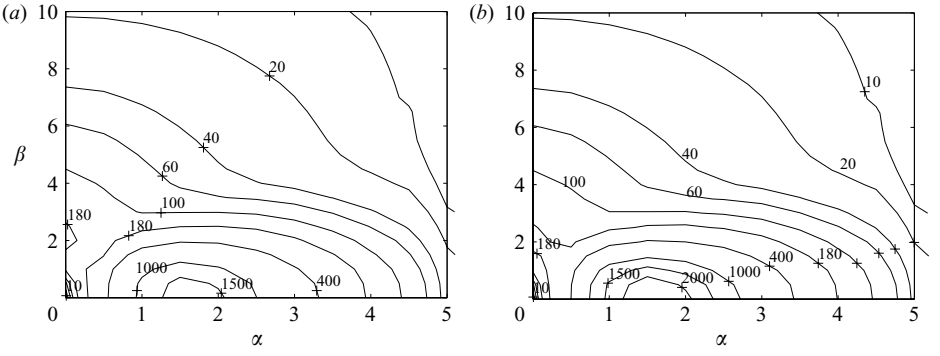

FIGURE 20. As figure 18, but for $Pr = 10^{-2}$. The new subcritical mode is now dominant at low Grashof number as well. The spanwise-independence of the largest transient growth, making the Poiseuille–Rayleigh–Bénard problem essentially two-dimensional, is unusual.

We now return to the question of how good a choice $B = 1$ is in (4.3). It is reasonable to assume that transient growth of disturbance kinetic energy and of temperature perturbations will each contribute to the growth of nonlinearities and hence to the later stages of transition, but direct numerical simulations or experiment are required to estimate their relative roles, i.e. to fix what value of B would correspond closest to reality. At extremely low Prandtl numbers, with $B \sim O(1)$ the contribution of the temperature perturbation to (4.3) is negligible compared to that of the kinetic energy. At extremely high Prandtl numbers, the reverse would be true, as has been verified from the eigenfunctions. In these limits, B will not affect the result even numerically, so long as it is $O(1)$. It is at $Pr \sim 1$ that the choice of B will matter most to the numerical value of the result. This expectation is borne out in figure 22, where the contour of G_{max} is plotted for two different Prandtl numbers, for $B = 0.2$, 1 and 2. At $Pr = 1$, the transient growth is smaller at smaller B, but the qualitative behaviour is the same. At $Pr = 7$, changing B has less of an effect. Here if the kinetic energy alone were to be considered, i.e. if B were set equal to 0, the transient growth is much smaller (not shown), but the biggest growth is still at $\beta = 0$. However, as discussed above, a non-zero B would be a more natural choice. Thus, our prediction that spanwise

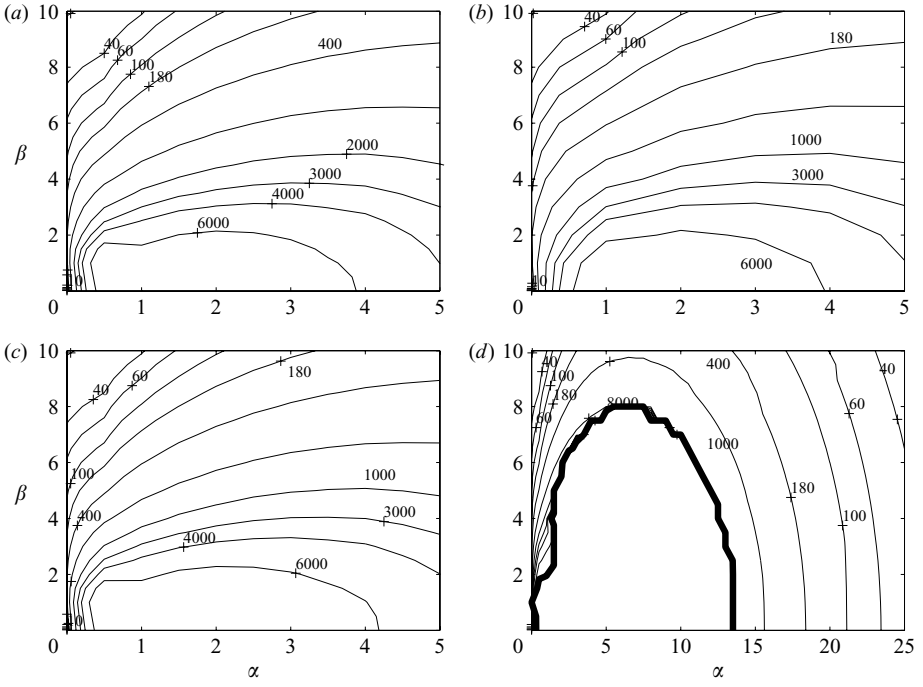

FIGURE 21. As figure 18, except that $Pr = 1$. (*a*) $Gr = 1$ (*b*) 10^2, (*c*) 10^3, (*d*) 10^4. The transient growth is even higher than before. The region inside the thick curve for $Gr = 10^4$ is linearly unstable.

independent structures and not streamwise streaks will dominate transient growth is robust and independent, within limits, of the choice of B. Finally, note that all computations of G_{max} are only indicative of how large the maximum possible transient growth can be, the actual numbers are not too significant, except in comparison to each other. Experimental estimates of transient growth are therefore much in order.

5. Secondary instability

A flow containing linear modes (either growing or decaying) of sufficient amplitude A_p can become unstable to new secondary modes of instability. Both transient disturbance growth and secondary instability require that the flow contain a non-negligible amplitude of the linear eigenmodes. However, secondary instabilities depend only on the least stable linear mode, and are exponentially growing, while optimum transient growth occurs only when several linear eigenmodes co-exist at appropriate amplitude ratios. In unheated channel flow, secondary instability is considered unimportant, since it it is believed to play a role only when external disturbance levels are extremely small. We show here that viscosity variations can significantly destabilize the secondary mode, thus making it more relevant to the transition process. The Prandtl number and Grashof number are set equal to zero.

The basic flow is now made up of two components, the steady laminar flow velocity $U(y)$ and the primary (linear) mode of instability $\hat{u}_p(x, y, z, t)$ obtained in the previous sections. A subscript p has been introduced in this section to denote the primary mode, to distinguish it from the secondary mode u_s. The primary mode is by definition (equation (3.1)) periodic in the streamwise and spanwise directions. In the regime of

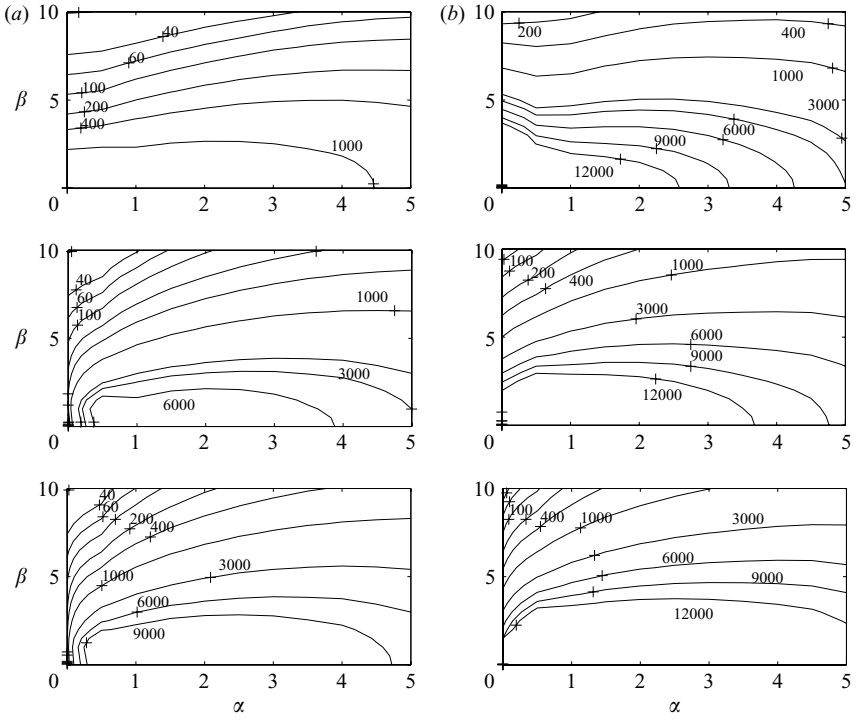

FIGURE 22. Effect of the choice of B in (4.3). The contour plot of G_{max} for $\Delta T = 25\,\mathrm{K}$, $Re = 1000$, asymmetric heating. (*a*) $Pr = 1$, (*b*) $Pr = 7$. From top to bottom the values of B are 0.2, 1 and 2 respectively.

interest, its rate of growth or decay is usually at least two orders of magnitude smaller than its frequency of oscillation. Thus, the new basic flow may be approximated to be periodic in time as well. A Floquet analysis, employing the standard approach as in Herbert (1983) and Bayly, Orszag & Herbert (1988), is carried out to study the stability of this flow. All flow variables are decomposed in the form

$$u(x, y, z, t) = U(y) + A_p \hat{u}_p(x, y, t) + A_s \hat{u}_s(x, y, z, t), \tag{5.1}$$

where A_s is the amplitude of the secondary. Note that with $Pr = 0$ and $Gr = 0$, Squire's transformation (Squire 1933) (substituting $\tilde{\alpha}^2 = \alpha^2 + \beta^2$ and $\tilde{\alpha}\tilde{Re} = \alpha Re$) can be applied to (3.2), to show that two-dimensional disturbances become unstable at the lowest Reynolds number when viscosity stratification alone is taken into consideration. The z-dependence of u_p is thus dropped in (5.1). The secondary perturbation quantities are assumed to be of the form

$$(\hat{u}_s, \hat{v}_s, \hat{w}_s) = \tfrac{1}{2}\left[(u_+, v_+, w_+)(y, t)\mathrm{e}^{\mathrm{i}(\alpha_+ x + \beta_+ z)} + (u_-, v_-, w_-)(y, t)\mathrm{e}^{\mathrm{i}(\alpha_- x + \beta_- z)} + \mathrm{c.c.}\right], \tag{5.2}$$

where α_+ and α_- are the wavenumbers of the secondary waves in the streamwise direction, and β_+ and β_- are the corresponding wavenumbers in the spanwise direction. Direct interactions between primary modes are assumed to be negligible, so nonlinear terms in the primary are dropped. Given the slow rate of decay, the variation of A_p over one cycle is neglected. The above decompositions are substituted into the momentum equations, the pressure is eliminated and nonlinear terms in the secondary disturbance are neglected. Then using the continuity equation, the streamwise component of secondary disturbance velocity is eliminated and we obtain

81 collocation points			161 collocation points		
ω_i	ω_r	β_s	ω_i	ω_r	β_s
0.000611	0.152931	0.50	0.000629	0.152943	0.50
0.017780	0.132593	1.00	0.017783	0.132595	1.00
0.013759	0.132595	2.00	0.013761	0.132595	2.00
0.007902	0.132595	3.00	0.007904	0.132595	3.00
0.002568	0.132595	4.00	0.002568	0.132595	4.00
−0.002646	0.132595	5.00	−0.002645	0.132595	5.00

TABLE 3. Sensitivity of the least stable eigenvalues to number of collocation points. The results are shown at $\alpha = 1.0$ and $m = 2.5$ for the symmetric profile with $Re = 5000$, $\alpha_+ = 0.5$ and $A_s = 0.01$. The convergence is better for smaller viscosity ratios.

secondary perturbation equations in v_+, v_-^*, w_+ and w_-^*. Upon suitable averaging over one wavelength in x and z and over one cycle in time, it is seen that only the resonant modes survive, which are related by

$$\alpha_+ + \alpha_- = \alpha, \qquad \beta_+ = -\beta_- = \beta_s. \tag{5.3}$$

The cases of $\alpha_+ = \alpha/2$ and $\alpha_+ = \alpha$ are called the subharmonic and the fundamental modes, respectively. The final equations for secondary stability are

$$-\mathrm{D}\frac{\partial v_+}{\partial t} + s\frac{\partial f_+}{\partial t} = -sAf_+ + (A\mathrm{D} - \mathrm{i}\alpha_+(\mathrm{D}U))v_+ - A_p\left[\frac{\mathrm{i}\alpha_+^2}{2\alpha_-}u_p\mathrm{D} + \frac{v_p\alpha_+\mathrm{D}^2}{2\alpha_-} + \frac{\mathrm{i}(\mathrm{D}u_p)\alpha_+}{2}\right]v_-^* + \frac{A_p\alpha_+^2}{2}\left[-v_p\mathrm{D} + \mathrm{i}\alpha_- u_p + \frac{\mathrm{i}\beta_s^2}{\alpha_-}u_p + \frac{\beta_s^2}{\alpha_+\alpha_-}v_p\mathrm{D}\right]f_-^*, \tag{5.4}$$

$$\frac{\partial v_+}{\partial t} - \mathrm{D}\frac{\partial f_+}{\partial t} = -Av_+ + (A\mathrm{D} + (\mathrm{D}A))f_+ - \frac{A_p(\alpha+\alpha_-)}{2}\left[\frac{v_p}{\alpha_-}\mathrm{D} - \mathrm{i}u_p\right]v_-^* + \frac{A_p}{2}\left[-\mathrm{i}(\alpha+\alpha_-)u_p\mathrm{D} - \mathrm{i}\alpha_-(\mathrm{D}u_p) + v_p\left(\frac{\alpha_+\beta_s^2}{\alpha_-} + \mathrm{D}^2\right)\right]f_-^*, \tag{5.5}$$

where $A = [\mathrm{i}\alpha_+ U + \mu s - \mu d^2 - \mu'\mathrm{D}]$, $f_+ = -(\mathrm{i}/\beta_s)w_+$ and $s = \alpha +^2 + \beta_s^2$, $\mathrm{D} = \mathrm{d}/\mathrm{d}y$. Equations (5.4) and (5.5) and the complementary equations for v_-^* and f_-^* are solved using a Chebyshev collocation spectral method, with the boundary conditions $\hat{u}_s, \hat{v}_s, \hat{w}_s = 0$ at $y = \pm 1$. The dispersion relation is $F(A_p, \beta_s, m, Re, \alpha, c,) = 0$ (see Herbert 1983). The growth rate is highly sensitive to the primary amplitude level A_p, and increases with increasing A_p. The present computations are validated by comparing with the unstratified case in Herbert (1983) as discussed in Sameen (2004). The agreement is excellent. The results are again obtained with 81 collocation points, and table 3 shows that doubling the number of collocation points does not change the answers much.

We first study asymmetric heating. A value of $A_p = 0.01$ is taken, to be representative of an intermediate level of primary disturbance. The variation of secondary growth rate ω_{is} with the spanwise wavenumber for various viscosity ratios is plotted in figure 23. As the temperature difference increases, a second highly unstable mode appears. This mode is three-dimensional, the spanwise and streamwise wavelengths being very close to each other. The modes which are closer to two-dimensional are now stabilized. A nonlinear or transient growth triggered by this new mode could

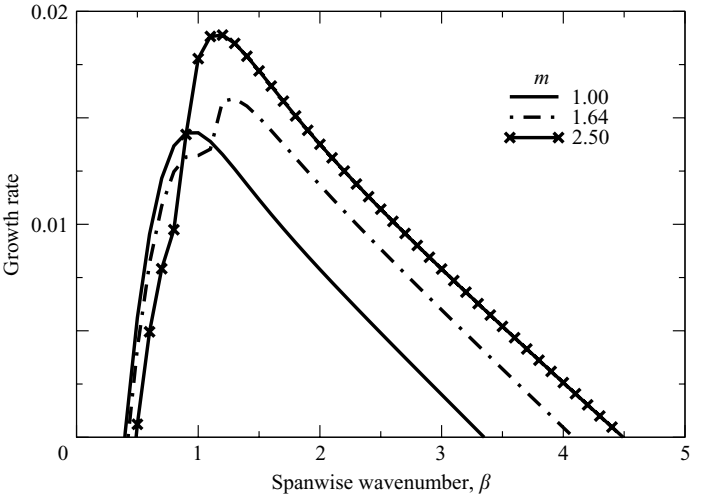

FIGURE 23. Dependence of growth rate on spanwise wavenumber of the secondary disturbance for various viscosity ratios, subharmonic case, asymmetric heating. $\alpha = 1.0$, $A_p = 0.01$, $Re = 5000$.

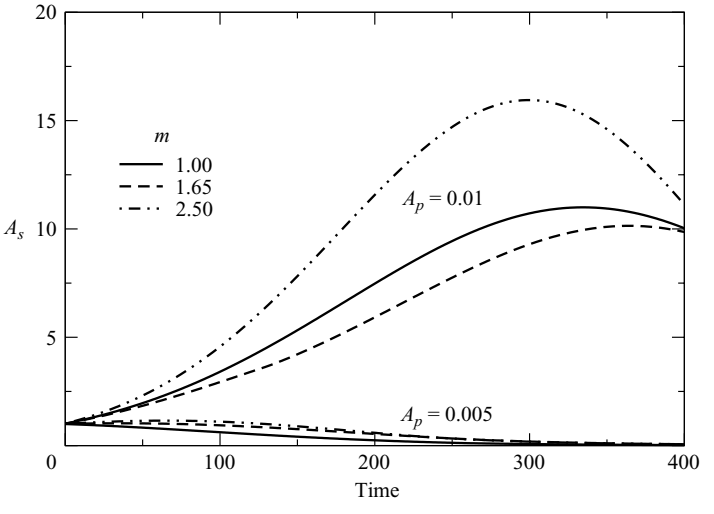

FIGURE 24. Variation with time of the amplitude of secondary disturbance for two sets of initial A_p. $\alpha = 1.0$, $\beta_s = 1.0$, $Re = 5000$, subharmonic mode, asymmetric heating.

mean that transition to turbulence proceeds somewhat differently, but further studies are required to evaluate this.

While we have taken the amplitude of the primary mode to be constant, it is in fact, at these Reynolds numbers, a known slowly decaying function of time. Integrating instantaneous results over long times, we can compute the time dependence of the amplitude of the secondary mode. This approach is a counterpart in time of the assumption of parallel flow in flows which vary slowly in x. The amplitude of the subharmonic secondary mode A_s is shown as a function of time in figure 24. At low initial A_p, secondary modes are always stable whereas for higher A_p significant growth is displayed up to large times. At low Reynolds number, the initial A_p required for

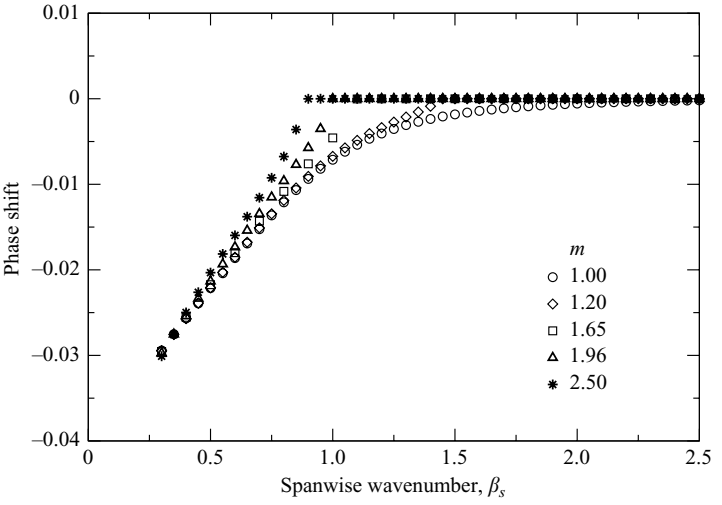

FIGURE 25. Variation of P_S with spanwise wavenumber for various viscosity ratios, subharmonic case, asymmetric heating. $\alpha = 1.0$, $A_p = 0.01$, $Re = 5000$.

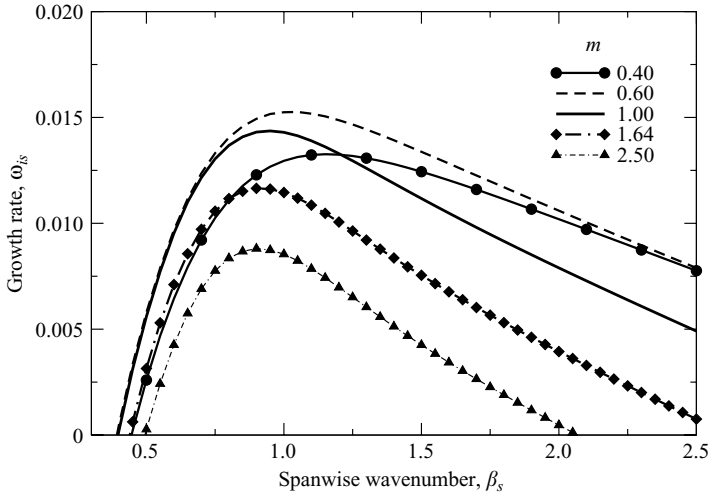

FIGURE 26. The dependence of growth rate on the spanwise wavenumber of the secondary disturbance for various viscosity ratios, subharmonic case. $\alpha = 1.0$, $A_p = 0.01$, $Re = 5000$, symmetric heating.

a sustained secondary instability growth is very high. In figure 25, the phase shift $P_S = \omega_p \alpha_+ / \alpha - \omega_s$ is shown as a function of the spanwise wavenumber. The phase locking of the subharmonic wave (i.e. where P_S is zero) is achieved at an earlier β_s than for the unstratified case.

It has been seen earlier that results from a symmetrically heated channel can be more intuitive than with asymmetric heating. For this reason, we examine this case. Figure 26 shows the secondary perturbation growth-rate variation with spanwise wavenumber β_s. A stabilization with increase in viscosity ratio, especially when $m > 1$, is evident. This behaviour is remarkable, being counterintuitive and opposite to the

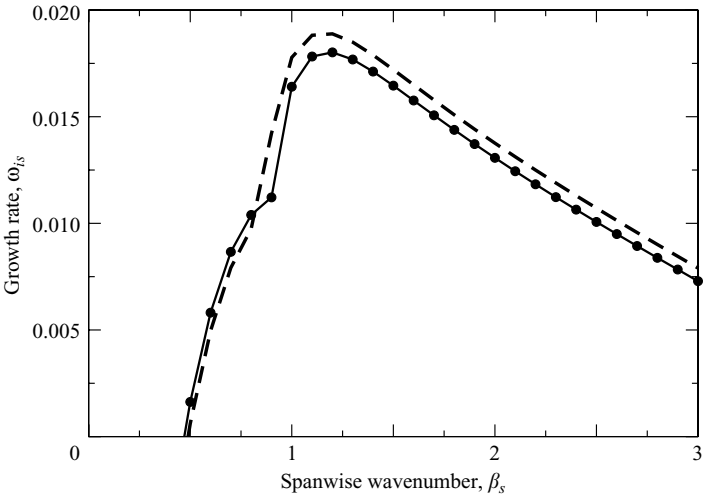

FIGURE 27. The new mode of instability arises from changes in the velocity profile. This is verified by switching off the viscosity gradient terms in the secondary stability equation. The dashed lines are for the full equation and the filled circles are with the viscosity gradient set to zero in the instability calculations, but retained in the mean flow computations. $\Delta T = 50(m = 2.5)$, $\alpha = 1.0$, $\alpha_s = 0.5$, $A_p = 0.01$, $Re = 5000$, asymmetric heating.

behaviour of the primary instability mode. The phase-locking behaviour is similar to the asymmetrically heated case.

We have seen that in linear disturbance growth, the mean velocity profile (via the U'' term) has a dominant role. In the case of secondary growth as well, Orszag & Patera (1983) have argued that inviscid effects are dominant, and act through vortex stretching and tilting. We are not able to make a conclusive statement on this, but it seems that heating affects secondary instability by an inviscid mechanism, through changes in the velocity profile. This is demonstrated in figure 27, where it is seen that switching off the viscosity gradient terms makes little difference to the result. Also, it is not evident why the sign of instability is opposite to that of primary modal growth. The inference here is that viscosity stratification alone can have unexpected effects on the various mechanisms leading to transition to turbulence.

6. Conclusion

In plane channel flow we have conducted a comprehensive study of the effect of heat, and show that there is no unique direction (either towards or away from stabilization) in which the flow responds. The linear stability results are in line with the findings of earlier studies. A decrease in viscosity as the wall is approached has a large stabilizing effect and vice versa. The effect on the linear eigenmode of reduced heat diffusion (increasing Prandtl number) is extremely small (Wall & Wilson 1996). Buoyancy has no effect up to a Grashof number of about 3000 and is enormously stabilizing or destabilizing thereafter, depending on the sign of the temperature difference. The Poiseuille–Rayleigh–Bénard and Tollmien–Schlichting modes are distinct at low Grashof number and merge at high Grashof numbers.

The effect of heat on transient growth of instabilities is unexpected. Viscosity stratification, which is the chief player in linear instability, has no discernible effect on this mechanism. Increasing Prandtl number, on the other hand, has an order of

magnitude destabilizing effect. Both of these are counter to the effect on the least stable linear mode. The assumption that Prandtl number may be neglected in stability analyses is therefore completely incorrect for this mechanism. Transient growth is also very high in the presence of buoyancy of the appropriate sign. With increasing Prandtl and/or Grashof number, the growth is two-dimensional, not in streamwise streaks, which is quite unusual for transient growth.

Secondary instabilities of the Tollmien–Schlichting modes are usually taken to be unimportant for channel-flow transition, but we find that viscosity-stratification can have a destabilizing effect on these modes, which may make them noticeable at large temperature differences.

It is hoped that this work with give impetus to experimental and computational studies to check these predictions and to explore wall heating in all its aspects as a control strategy for channel and pipe flows.

We are indebted to Professor O. N. Ramesh for discussions throughout the course of this work and for reading the manuscript. A part of the work was carried out during the tenure of A. S. as a PhD student at the Indian Institute of Science. R. G. would like to thank the Director, NPOL for supporting a part of the work and Dr Rao Tatavarti for his constant encouragement.

REFERENCES

Bayly, B. J., Orszag, S. A. & Herbert, T. 1988 Instability mechanisms in shear-flow transition. *Annu. Rev. Fluid Mech.* **20**, 359–391.

Biau, D. & Bottaro, A. 2004 The effect of stable thermal stratification on shear flow instability. *Phys. Fluids* **16** (14), 4742–4745.

Canuto, C., Hussaini, M. Y., Quarteroni, A. & Zang, T. A. 1987 *Spectral Methods in Fluid Dynamics*, 1st edn. Springer.

Carriere, P. & Monkewitz, P. A. 1999 Convective versus absolute instability in mixed Rayleigh–Benard–Poiseuille convection. *J. Fluid Mech.* **384**, 243–262.

Chandrasekhar, S. 1961 *Hydrodynamics and Hydromagnetic Stability*. Oxford University Press.

Chikkadi, V. K., Sameen, A. & Govindarajan, R. 2005 Preventing transition to turbulence: viscosity stratification will not always help. *Phys. Rev. Lett.* **95**, 264504.

Corbett, P. & Bottaro, A. 2001 Optimal linear growth in swept boundary layers. *J. Fluid Mech.* **435**, 1–23.

Criminale, W. O., Jackson, T. L. & Joslin, R. D. 2003 *Theory and Computation in Hydrodynamic Stability*. Cambridge University Press.

Davies, S. J. & White, C. M. 1928 An experimental study of the flow of water in pipes of rectangular section. *Proc. R. Soc. Lond.* **119**, 92–107.

Deardorff, J. W. 1965 Gravitational instability between horizontal plates with shear. *Phys. Fluids* **8** (6), 1027–1030.

Faisst, H. & Eckhardt, B. 2003 Traveling waves in pipe flow. *Phys. Rev. Lett.* **91**, 224502.

Foster, R. 1997 Structure and energetics of optimal Ekman layer perturbations. *J. Fluid Mech.* **333**, 97–123.

Fujimura, K. & Kelly, R. E. 1988 Stability of unstably stratified shear flow between parallel plates. *Fluid Dyn. Res.* **2**, 281–292.

Gage, K. S. 1971 The effect of stable thermal stratification on the stability of viscous parallel flow. *J. Fluid Mech.* **47**, 1–20.

Gage, K. S. & Reid, W. H. 1968 The stability of thermally stratified plane Poiseuille flow. *J. Fluid Mech.* **33**, 21–32.

Hanifi, A. & Henningson, D. S. 1998 The compressible inviscid algebraic instability for streamwise independent disturbances. *Phys. Fluids* **10**, 1784.

Hanifi, A., Schmid, P. J. & Henningson, D. S. 1996 Transient growth in compressible boundary layer flow. *Phys. Fluid* **8**, 826–837.

Herbert, T. 1983 Secondary instability of plane channel flow to subharmonic three-dimensional disturbances. *Phys. Fluids* **26** (4), 871–874.

Hof, B., van Doorne, C. W. H., Westerweel, J., Nieuwstadt, F. T. M., Faisst, H., Eckhardt, B., Wedin, H., Kerswell, R. R. & Waleffe, F. 2004 Experimental observation of nonlinear traveling waves in turbulent pipe flow. *Science* **305**, 1594–1598.

Kao, T. W. 1968 Role of viscosity stratification in the stability of two-layer flow down an incline. *J. Fluid Mech.* **33**, 561–572.

Kao, T. W. & Park, C. 1970 Experimental investigations of the stability of channel flows. Part 1. Flow of a single liquid in a rectangular channel. *J. Fluid Mech.* **43**, 145–164.

Kerswell, R. R. 2005 Recent progress in understanding the transition to turbulence in pipe. *Nonlinearity* **18**, R17–R44.

Landahl, M. T. 1980 A note on an algebraic instability of inviscid parallel shear flows. *J. Fluid Mech.* **98**, 243–251.

Lauchle, G. & Gurney, G. 1984 Laminar boundary-layer transition on a heated underwater body. *J. Fluid Mech.* **144**, 79–101.

Lide, D. R. 1999 *CRC Handbook of Chemistry and Physics*, 79th edn. CRC press.

Liepmann, H. W. & Fila, G. H. 1947 Investigations of effects of surface temperature and single roughness elements on boundary-layer transition. *NACA TN* 1196.

Mahajan, R. L., Gebhart, B., Sammakia, B. & Jaluria, Y. 1988 *Buoyancy Induced Flows and Transport*. Taylor & Francis.

Malik, V. S. & Hooper, P. A. 2005 Linear stability and energy growth of viscosity stratified flows. *Phys. Fluids* **17**, 024101.

Meseguer, A. 2002 Energy transient growth in the Taylor–Couette problem. *Phys. Fluids* **14** (5).

Morkovin, M. V. & Reshotko, K. 1989 Dialogue on progress and issues in stability and transition research. *IUTAM Symp. on Laminar–Turbulent Transition*, pp. 3–29.

Narayanan, M. A. B. & Narayanan, T. 1967 *Z. Angew. Math. Phys.* **18**, 642.

Orszag, S. & Patera, A. 1983 Secondary instability of wall-bounded shear flows. *J. Fluid Mech.* **128**, 347–385.

Orszag, S. A. 1971 Accurate solution of the Orr–Sommerfeld stability equation. *J. Fluid Mech.* **50**, 689–703.

Patel, V. C. & Head, M. R. 1969 Some observations on skin friction and velocity profiles in fully developed pipe and channel flows. *J. Fluid Mech.* **38**, 181–201.

Peyret, R. 2002 *Spectral Methods for Incompressible Viscous Flow*. Springer.

Pinarbasi, A. & Liakopoulos, A. 1995 Role of variable viscosity in the stability of channel flow. *Intl Commun. Heat Mass Transfer* **22**, 837–847.

Platten, J. K. & Legros, J. C. 1984 *Convection in Liquids*. Springer.

Potter, M. C. & Graber, E. 1972 Stability of plane Poiseuille flow with heat transfer. *Phys. Fluids* **15**, 387.

Reddy, S. C. & Henningson, D. S. 1993 Energy growth in viscous channel flows. *J. Fluid Mech.* **252**, 209–238.

Reddy, S. C. & Henningson, D. S. 1994 On the role of linear mechanisms in transition to turbulence. *Phys. Fluids* **6**, 1396.

Reddy, S. C., Schmid, P. J., Bagget, J. S. & Henningson, D. S. 1998 On stability of streamwise streaks and transition thresholds in plane channel flows. *J. Fluid Mech.* **365**, 269–303.

Sameen, A. 2004 Stability of plane channel flow with viscosity-stratification. PhD thesis, Dept. of Aerospace Engng, Indian Institute of Science.

Schafer, P. & Herwig, H. 1993 Stability of plane Poiseuille flow with temperature dependent viscosity. *Intl J. Heat Mass Transfer* **36**, 2441–2448.

Schafer, P., Severin, J. & Herwig, H. 1995 The effect of heat transfer on the stability of laminar boundary layers. *Intl J. Heat Mass Transfer* **38**, 1855.

Schmid, P. J. & Henningson, D. S. 2001 *Stability and Transition in Shear Flows*. Springer.

Squire, H. B. 1933 On the stability of three-dimensional disturbance of viscous flow between parallel walls. *Proc. R. Soc.* A **142** (621–8), 129.

Strazisar, A. J., Reshotko, E. & Prahl, J. M. 1977 Experimental study of the stability of heated laminar boundary layer in water. *J. Fluid Mech.* **83**, 225–247.

Turner, J. S. 1959 Buoyant plumes and thermals. *Annu. Rev. Fluid Mech.* **1**, 29–44.

Tveitereid, M. 1974 On the stability of thermally stratified plane Poiseuille flow. *Z. Angew. Math. Mech.* **54**, 533–540.

Waleffe, F. 1995 Transition in shear flows. Nonlinear normality versus non-normal linearity. *Phys. Fluids* **7**, 3060.

Waleffe, F. 1997 On a self-sustaining process in shear flows. *Phys. Fluids* **9**, 883–900.

Wall, D. P. & Wilson, S. K. 1996 The linear stability of channel flow of fluid with temperature-dependent viscosity. *J. Fluid Mech.* **323**, 107–132.

Wazzan, A. R., Okamura, T. T. & Smith, A. M. O. 1968 The stability of water flow over heated and cooled flat plates. *Trans. ASME* C: *J. Heat Transfer* **99**, 109–114.

Zhang, J., Childress, S. & Libchaber, A. 1998 Non-Boussinesq effect: asymmetric velocity profiles in thermal convection. *Phys. Fluids* **10**, 1534–1536.